

Theoretical Modeling of ME effect at Low frequency and Resonance Frequency for Magnetolectric Laminates with Anisotropic Piezoelectric Properties.

Deepak Rajaram Patil^{1,a)}, Yisheng Chai^{1,a)}, Rahul C. Kambale², Byung-Gu Jeon¹, Jungho Ryu^{2,b)}, Woon-Ha Yoon², Dong-Soo Park², Dae-Yong Jeong³, Sang-Goo Lee⁴, Jeongho Lee⁴, Joong-Hee Nam⁵, Jeong-Ho Cho⁵, Byung-Ik Kim⁵, and Kee Hoon Kim^{1,b)}

¹CeNSCMR, Department of Physics and Astronomy, Seoul National University, Seoul 151-747, Republic of Korea.

²Functional Ceramics Group, Korea Institute of Materials Science (KIMS), 66 Sangnam-Dong, Changwon, Gyeongnam 641–831, Republic of Korea.

³School of Materials Engineering, Inha University, Incheon 402-751, Korea.

⁴iBULe Photonics Co. Ltd, 7-39 Songdo-dong Yeonsu-gu Incheon, Korea.

⁵Center for Electronic Component Research, Korea Institute of Ceramic Engineering and Technology, Seoul 153-801, Republic of Korea

^{a)}D. R. Patil and Y. S. Chai contributed equally to this work.

^{b)}Author to whom correspondence should be addressed.

Electronic mail:khkim@phy.snu.ac.kr, jhryu@kims.re.kr

ABSTRACT:

A new theory is developed for the magnetoelectric (ME) coupling in a symmetric 2-2 ME laminate having a representative piezoelectric crystal (PMN-PT) particularly with anisotropic piezoelectric properties. Considering the average field method, the theoretical expressions for the transverse ME voltage coefficients at low and resonance frequencies were derived. The theory takes into account the anisotropic properties of the piezoelectric materials providing two different expressions of transverse ME voltage coefficients for different in-plane magnetic fields both at low and resonance frequencies. The numerical simulations show multiple resonance frequencies and phase difference between transverse ME voltage coefficients showing good agreement with the experimental results. Our theory should be generally applicable to other ME laminates with any piezoelectrics with anisotropic piezoelectric coefficients.

I. INTRODUCTION:

Multiferroic materials offer a unique capability of cross-control of polarization (P) by a magnetic field (H) or of magnetization (M) by an electric field (E), which is designated as the magnetoelectric (ME) effect.^{1,2} The ME effect has a great potential for many device applications such as energy harvesters, field sensors, gyrators, and transducers.³⁻⁶ Since the intrinsic ME response in single-phase ME materials is very low to be utilized for device application, there have been significant progresses in recent years focused on the extrinsic ME coupling in ME composites composed of magnetostrictive and piezoelectric materials.⁷⁻¹³ The ME effect in ME composites is an extrinsic product property relies on two step process: magnetic field induced mechanical strain via magnetostriction and stress-induced electric field via piezoelectric effect. The ME effect is expressed in terms of ME coefficient $\alpha = \delta P / \delta H$, which is related to the ME voltage coefficient, $\alpha_E = \delta E / \delta H$ by relation $\alpha = \epsilon_0 \epsilon_r \alpha_E$, where ϵ_r is the relative permittivity of the material. Intensive experimental and theoretical studies have been done to improve the ME coupling by using numerous material combinations with superior striction properties or better interface coupling by using different connectivity schemes (e.g., 0-3, 2-2, 1-3, 1-2).⁷⁻¹³ More recent approaches to multiferroic composites explore the utilization of the metglas and $\text{Pb}(\text{Mg}_{1/3}\text{Nb}_{2/3})\text{O}_3\text{-PbTiO}_3$ (PMN-PT) or related piezoelectric materials, because of their superior ME coupling.¹⁴⁻¹⁸ Based on this new approach, a milestone in the development of ME composites was the appearance of 1-2 structure using a piezofiber layer of PMN-PT sandwiched between two FeBSiC alloy layers, giving rise to record high values of 45 V/cmOe at off-resonance and 1100 V/cmOe at resonance.¹⁴

Theoretically, different methods have been proposed for ME effect both at low frequency and resonance frequencies, including average field, equivalent circuit and Green function.^{7-9,19-23}

Theoretically it has been predicted that the 2–2 connectivity in laminates shows highest ME coupling amongst the various composite systems. However, the predicted values showed several times higher magnitude of ME voltage coefficient than the experimental values, which is possibly due to the consideration of a one-dimensional (1D) approach. The 1D approach only considers the internal stresses along the length direction while ignoring the transverse stresses along the width direction. In this respect recently, Wang *et.al*²⁴ has developed an analytical model for ME coupling at low frequency based on an average-field method by considering the geometry effect. They found that the predicted ME coefficient depended not only on the parameters of the components but also on the composite geometry. Similarly Bao and Luo²⁵ were developed a theoretical model for ME effect at resonance frequency considering the 2D stresses. They proved that the theoretical results based on 2D stresses are in better agreement with the experimental data compared with that of 1D stresses theory.

However, we note that until now, almost all the theoretical models are based on the symmetric 2-2 laminates composed of the magnetostrictive and piezoelectric phases having isotropic in-plane striction properties. All these theoretical models have considered the isotropic piezoelectric coefficients ($d_{31}=d_{32}$) and elastic compliances ($s_{11}^p = s_{22}^p$) for the piezoelectric phase, which resulted in the isotropic stress and strain components along different in-plane directions, which in turn resulted in the isotropic transverse ME voltage coefficients i.e., $\alpha_{E31} = \alpha_{E32}$. In contrast, if the piezoelectric phase with anisotropic piezoelectric coefficients i.e., ($d_{31} = -d_{32}$) and elastic compliances ($s_{11}^p \neq s_{22}^p$) is adopted, one can expect the opposite transverse stress and strain components along different in-plane directions, which could result in the anisotropic transverse ME voltage coefficients at both low and resonance frequencies. Recently, we have indeed shown the giant enhancement and strong anisotropy in the transverse ME voltage coefficients for 2-2

type symmetric metglas/PMN-PT/metglas ME laminate owing to the anisotropic transverse piezoelectric properties of [011] oriented PMN-PT crystal. However, we found that a theoretical analysis is needed for the clear understanding of the anisotropic giant ME coupling in these composites.

Herein, we present a new theory for the ME coupling in a symmetric 2-2 laminate having a piezoelectric crystal with anisotropic piezoelectric properties. The theoretical expressions for the transverse ME voltage coefficients at low and resonance frequencies were derived by using average field theory. The theoretical simulations data showed multiple resonance frequencies and phase difference in transverse ME voltage coefficients likely due to the anisotropic piezoelectric properties. The theoretical results have been compared to the experimental results, which show good agreement with each other.

II. THEORETICAL MODELING:

1. ME effect at low frequency:

Let us consider a layered composite structure consisting of n -layer piezoelectric with anisotropic piezoelectric properties ($d_{31} \neq d_{32}$ and $s_{11}^p \neq s_{22}^p$)²⁶ and $n+1$ layer of magnetostrictive phase, as shown in Fig. 1(a), which has the form of a thin plate with length l and width w .

The constitutive equations for the strain components S_i^m and S_i^p of the magnetic and piezoelectric layers and the electric displacement D_3 of the piezoelectric layer can be written as,

$$S_1^p = s_{11}^p T_1^p + s_{21}^p T_2^p + d_{31}^p E_3$$

$$S_2^p = s_{12}^p T_1^p + s_{22}^p T_2^p + d_{32}^p E_3$$

$$S_1^m = s_{11}^m T_1^m + s_{21}^m T_2^m + q_{11}^m H_1$$

$$S_2^m = s_{12}^m T_1^m + s_{22}^m T_2^m + q_{12}^m H_1$$

$$D_3 = d_{31}^p T_1^p + d_{32}^p T_2^p + \epsilon_{33}^T E_3 \quad (1)$$

Here, T_i^p are the stress components in the piezoelectric phase, s_{ij}^p are the compliance coefficients of the piezoelectric phase under constant stress, T_i^m are the stress components in the magnetostrictive phase, s_{ij}^m are the compliance coefficients of the piezoelectric phase under constant stress, ϵ_{33}^T is the permittivity, d_{31}^p and d_{32}^p are the piezoelectric coefficients, q_{11}^m and q_{12}^m are the piezomagnetic coefficients, and E_3 and H_1 are the electric and magnetic field strengths.

Considering the internal stresses within magnetostrictive and piezoelectric plates with the perfect interface coupling i.e. $k=1$ and according to Newton's third law, we get following relationships about the internal forces between layers:

$$fT_1^m + (1-f)T_1^p = 0, \quad fT_2^m + (1-f)T_2^p = 0 \quad (2)$$

Where, f denotes the volume fraction of the magnetostrictive phase in the ME laminate and is equal to 0.5 in our laminates.

For the solutions of Eq. (2), the following boundary conditions were used:

$$T_1^p = -T_1^m, \quad T_2^p = -T_2^m, \quad S_1^p = S_1^m, \quad S_2^p = S_2^m \quad (3)$$

Combining Eqs. (1), (2) and (3), we can obtain

$$\begin{aligned} T_1^p &= [\underline{s_{22}}(q_{11}^m H_1 - d_{31}^p E_3) - \underline{s_{21}}(q_{12}^m H_1 - d_{32}^p E_3)] / 2[\underline{s_{11}}\underline{s_{22}} - \underline{s_{21}}\underline{s_{12}}] \\ T_2^p &= [\underline{s_{11}}(q_{12}^m H_1 - d_{32}^p E_3) - \underline{s_{12}}(q_{11}^m H_1 - d_{31}^p E_3)] / 2[\underline{s_{11}}\underline{s_{22}} - \underline{s_{21}}\underline{s_{12}}] \end{aligned} \quad (4)$$

where, the effective compliance coefficients were defined as,

$$\underline{s}_{22} = \frac{(s_{22}^p + s_{22}^m)}{2}, \underline{s}_{21} = \frac{(s_{21}^p + s_{21}^m)}{2}$$

$$\underline{s}_{11} = \frac{(s_{11}^p + s_{11}^m)}{2}, \underline{s}_{12} = \frac{(s_{12}^p + s_{12}^m)}{2}$$

Magnetolectric coupling is estimated from the induced field δE across the sample that is subjected to an ac magnetic-field δH in the presence of a bias field H_{dc} . Basic relations for transverse ME coefficients are obtained for two orientations of H_{dc} and δH i.e. along direction 1 or along direction 2. From Eqs. (1) and (4), and considering the open circuit condition $D_3=0$, the transverse ME coefficient $\alpha_{E31} = \delta E_3 / \delta H_1$ can be expressed as,

$$\alpha_{E31} = \frac{(d_{31}^p \underline{s}_{22} q_{11}^m + d_{32}^p \underline{s}_{11} q_{12}^m) - \underline{s}_{21} (d_{31}^p q_{12}^m + d_{32}^p q_{11}^m)}{2\varepsilon_{33}^p [\underline{s}_{11} \underline{s}_{22} - (\underline{s}_{21})^2] - [\underline{s}_{22} (d_{31}^p)^2 + \underline{s}_{11} (d_{32}^p)^2 - 2\underline{s}_{21} d_{31}^p d_{32}^p]} \quad (5)$$

Similarly, the transverse ME coefficient $\alpha_{E32} = \delta E_3 / \delta H_2$ can be expressed as,

$$\alpha_{E32} = \frac{(d_{31}^p \underline{s}_{22} q_{21}^m + d_{32}^p \underline{s}_{11} q_{22}^m) - \underline{s}_{21} (d_{31}^p q_{22}^m + d_{32}^p q_{21}^m)}{2\varepsilon_{33}^p [\underline{s}_{11} \underline{s}_{22} - (\underline{s}_{21})^2] - [\underline{s}_{22} (d_{31}^p)^2 + \underline{s}_{11} (d_{32}^p)^2 - 2\underline{s}_{21} d_{31}^p d_{32}^p]} \quad (6)$$

One can check the validity of the above equations by solving the above equations for isotropic 2D laminate with isotropic piezoelectric properties. After putting the isotropic piezoelectric material parameters $s_{11}^p = s_{22}^p, s_{12}^p = s_{21}^p, d_{31}^p = d_{32}^p$ in the Eqs. (5) and (6) one can get,

$$\alpha_{E31} = -\frac{kf(1-f)d_{31}(q_{11} + q_{21})}{\varepsilon_{33} \underline{s}_{11} - 2kfd_{31}^2} \quad (7)$$

where, $\underline{s}_{11} = f(s_{11}^p + s_{12}^p) + k(1-f)(s_{11}^m + s_{12}^m)$.⁸ Note that α_{E32} has the same form of Eq. (7)

and $\alpha_{E31} = \alpha_{E32}$ holds in the isotropic piezoelectric/magnetostrictive media as the equality relations of $d_{31} = d_{32}, q_{11} = q_{22}$ and $q_{12} = q_{21}$ are valid.

2. ME effect at resonance frequency:

The ME effect in the composites is driven by the mechanical coupling between the piezoelectric and magnetic phases, the ME effect would be greatly enhanced when the piezoelectric or magnetic phase undergoes mechanical resonance i.e., an electromechanical resonance (EMR) for the piezoelectric phase and ferromagnetic resonance (FMR) for the magnetic phase. Since the ME equations for α_{E31} and α_{E32} at low frequency show anisotropy for different in-plane H , one can expect the same anisotropy for α_{E31} and α_{E32} at resonance conditions. Therefore it is equally important to understand the theoretical modelling for the transverse ME voltage coefficient at resonance by solving the fundamental constitutive equations. In order to describe the ME voltage coefficient at resonance conditions we need the equations of elastodynamics along with the above fundamental constitutive equations.

From Eqs. (1) and (3) the following equations for the effective parameters for the composites can be derived:

$$S_1^p = s_{11}^p T_1^p + q_{11}^m H_1 + d_{31}^p E_3,$$

$$S_2^p = s_{22}^p T_2^p + q_{12}^m H_1 + d_{32}^p E_3,$$

$$S_1^m = s_{11}^m T_1^m + d_{31}^p E_3 + q_{11}^m H_1,$$

$$S_2^m = s_{22}^m T_2^m + d_{32}^p E_3 + q_{12}^m H_1,$$

$$T_1^p = \frac{(s_{22}^p S_1^p - s_{21}^p S_2^p)}{(s_{11}^p s_{22}^p - s_{21}^p s_{12}^p)} - \frac{E_3 (s_{22}^p d_{31}^p - s_{21}^p d_{32}^p)}{(s_{11}^p s_{22}^p - s_{21}^p s_{12}^p)}$$

$$T_2^p = \frac{(s_{12}^p S_1^p - s_{11}^p S_2^p)}{(s_{21}^p s_{12}^p - s_{11}^p s_{22}^p)} - \frac{E_3 (s_{12}^p d_{31}^p - s_{11}^p d_{32}^p)}{(s_{21}^p s_{12}^p - s_{11}^p s_{22}^p)}$$

$$\begin{aligned}
D_3 &= d_{31}^p T_1^p + d_{32}^p T_2^p + \varepsilon_{33}^T E_3 \\
&= \left[\frac{d_{31}^p (s_{22}^p S_1^p - s_{21}^p S_2^p)}{(s_{11}^p s_{22}^p - s_{21}^p s_{12}^p)} - \frac{d_{31}^p E_3 (s_{22}^p d_{31}^p - s_{21}^p d_{32}^p)}{(s_{11}^p s_{22}^p - s_{21}^p s_{12}^p)} \right] + \left[\frac{d_{32}^p (s_{11}^p S_2^p - s_{12}^p S_1^p)}{(s_{11}^p s_{22}^p - s_{21}^p s_{12}^p)} - \frac{d_{32}^p E_3 (s_{11}^p d_{32}^p - s_{12}^p d_{31}^p)}{(s_{11}^p s_{22}^p - s_{21}^p s_{12}^p)} \right] + \varepsilon_{33}^T E_3 \\
&= \left[\frac{S_1^p (d_{31}^p s_{22}^p - d_{32}^p s_{12}^p) - S_2^p (d_{31}^p s_{21}^p - d_{32}^p s_{11}^p)}{(s_{11}^p s_{22}^p - s_{21}^p s_{12}^p)} \right] + E_3 \left(\varepsilon_{33}^T - \frac{s_{22}^p (d_{31}^p)^2 + s_{11}^p (d_{32}^p)^2 - (s_{12}^p + s_{21}^p) d_{31}^p d_{32}^p}{(s_{11}^p s_{22}^p - s_{21}^p s_{12}^p)} \right)
\end{aligned} \tag{8}$$

$$\text{where, } s_{11}^{p'} = \frac{s_{11}^p s_{21}^m - s_{11}^m s_{12}^p}{s_{21}^m + s_{12}^p}, \quad s_{22}^{p'} = \frac{s_{12}^p s_{22}^m - s_{12}^m s_{22}^p}{s_{12}^m + s_{12}^p}, \quad d_{31}^{p'} = d_{31}^p \frac{s_{21}^m}{s_{21}^m + s_{12}^p}, \quad d_{32}^{p'} = d_{31}^p \frac{s_{12}^m}{s_{12}^m + s_{12}^p}$$

$$s_{11}^{m'} = \frac{s_{11}^m s_{12}^p - s_{11}^p s_{21}^m}{s_{12}^p + s_{21}^m}, \quad s_{22}^{m'} = \frac{s_{12}^p s_{22}^m - s_{11}^m s_{22}^p}{s_{12}^p + s_{21}^m}, \quad q_{11}^{m'} = q_{11}^m \frac{s_{12}^p}{s_{12}^p + s_{21}^m}, \quad q_{12}^{m'} = q_{12}^m \frac{s_{12}^p}{s_{12}^p + s_{21}^m}$$

Based on the coordinate system shown in **Fig. 1(a)**, and applying Newton's second law to the ME element, the equations of motion for any mass element oriented in the direction of the x and y axis can be respectively written as,

$$\begin{aligned}
\frac{\partial^2 u}{\partial x^2} + k_x^2 u &= 0, \\
\frac{\partial^2 v}{\partial y^2} + k_y^2 v &= 0
\end{aligned} \tag{9}$$

Where u, v are the displacements of the mass element for the magnetolectric element along x and y axis. The wave numbers k_x and k_y is given by:

$$k_x = \omega / \sqrt{\left(\frac{1-f}{s_{11}^p} + \frac{f}{s_{11}^m} \right) / \bar{\rho}}, \quad k_y = \omega / \sqrt{\left(\frac{1-f}{s_{22}^p} + \frac{f}{s_{22}^m} \right) / \bar{\rho}}$$

$\bar{\rho} = f \rho_m + (1-f) \rho_p$ is the average mass density, where ρ_p and ρ_m represent the densities of the piezoelectric and magnetostrictive materials, respectively.

The solutions of Eq. (9) can be written as:

$$\begin{aligned}
u &= A_u \sin(k_x u) + B_u \cos(k_x u) \\
v &= A_v \sin(k_y u) + B_v \cos(k_y u)
\end{aligned}
\tag{10}$$

To determine A_u, A_v, B_u and B_v , according to Eq. (8):

$$S_1^p = \frac{\partial u}{\partial x} = s_{11}^{p'} T_1^p + q_{11}^{m'} H_1 + d_{31}^{p'} E_3, \tag{11}$$

$$S_2^p = \frac{\partial v}{\partial y} = s_{22}^{p'} T_2^p + q_{12}^{m'} H_1 + d_{32}^{p'} E_3 \tag{12}$$

In free boundary conditions, when $u = 0$ or l and $v = 0$ or w , T_1^p and T_2^p will become zero, which gives:

$$\begin{aligned}
B_u &= \frac{q_{11}^{m'} H_1 + d_{31}^{p'} E_3}{k_x}, B_v = \frac{q_{12}^{m'} H_1 + d_{32}^{p'} E_3}{k_x} \\
A_u &= B_u \frac{\cos(k_x l) - 1}{\sin(k_x l)}, A_v = B_v \frac{\cos(k_y w) - 1}{\sin(k_y w)}
\end{aligned}
\tag{13}$$

Putting Eq. (13) back to Eq. (10) and taking derivative, one can obtain:

$$\begin{aligned}
S_1^p &= \frac{\partial u}{\partial x} = (q_{11}^{m'} H_1 + d_{31}^{p'} E_3) \frac{[\sin(k_x(l-x)) + \sin(k_x x)]}{\sin(k_x l)} \\
S_2^p &= \frac{\partial v}{\partial y} = (q_{12}^{m'} H_1 + d_{32}^{p'} E_3) \frac{[\sin(k_y(w-y)) + \sin(k_y y)]}{\sin(k_y w)}
\end{aligned}
\tag{14}$$

The ME voltage coefficient is determined using the open circuit condition:

$$\int_0^w \int_0^l D_3 dx dy = 0 \tag{15}$$

Substituting Eq. (8) into (15):

$$\begin{aligned}
\int_0^w \int_0^l D_3 dx dy &= \int_0^w \int_0^l \left(\left[\frac{S_1^p (d_{31}^p s_{22}^p - d_{32}^p s_{12}^p) - S_2^p (d_{31}^p s_{21}^p - d_{32}^p s_{11}^p)}{(s_{11}^p s_{22}^p - s_{21}^p s_{12}^p)} \right] + E_3 \left(\epsilon_{33}^T - \frac{s_{22}^p (d_{31}^p)^2 + s_{11}^p (d_{32}^p)^2 - (s_{12}^p + s_{21}^p) d_{31}^p d_{32}^p}{(s_{11}^p s_{22}^p - s_{21}^p s_{12}^p)} \right) \right) dx dy \\
&= \left(\left[\frac{(d_{31}^p s_{22}^p - d_{32}^p s_{12}^p) \int_0^w \int_0^l S_1^p dx dy - (d_{31}^p s_{21}^p - d_{32}^p s_{11}^p) \int_0^w \int_0^l S_2^p dx dy}{(s_{11}^p s_{22}^p - s_{21}^p s_{12}^p)} \right] + l w E_3 \left(\epsilon_{33}^T - \frac{s_{22}^p (d_{31}^p)^2 + s_{11}^p (d_{32}^p)^2 - (s_{12}^p + s_{21}^p) d_{31}^p d_{32}^p}{(s_{11}^p s_{22}^p - s_{21}^p s_{12}^p)} \right) \right) \tag{16}
\end{aligned}$$

Substituting S_1^p and S_2^p terms from Eq. (14) into (16):

$$\int_0^w \int_0^l S_1^p dx dy = (q_{11}^{m'} H_1 + d_{31}^{p'} E_3) w \int_0^l \frac{[\sin(k_x(l-x)) + \sin(k_x x)]}{\sin(k_x l)} dx = \frac{2(q_{11}^{m'} H_1 + d_{31}^{p'} E_3) w}{k_x \cot \frac{k_x l}{2}}$$

$$\int_0^w \int_0^l S_2^p dx dy = (q_{12}^{m'} H_1 + d_{32}^{p'} E_3) l \int_0^w \frac{[\sin(k_y(w-y)) + \sin(k_y y)]}{\sin(k_y w)} dy = \frac{2(q_{12}^{m'} H_1 + d_{32}^{p'} E_3) l}{k_y \cot \frac{k_y w}{2}} \quad (17)$$

Finally, the transverse ME coefficient $\alpha_{E31} = \delta E_3 / \delta H_1$ is given by:

$$\alpha_{E31} = \frac{\left(\frac{2q_{11}^{m'}(d_{32}^p s_{12}^p - d_{31}^p s_{22}^p)}{k_x l \cot(k_x l / 2)} + \frac{2q_{12}^{m'}(d_{31}^p s_{21}^p - d_{32}^p s_{11}^p)}{k_y w \cot(k_y w / 2)} \right)}{\left(\frac{2d_{31}^{p'}(d_{31}^p s_{22}^p - d_{32}^p s_{12}^p)}{k_x l \cot(k_x l / 2)} + \frac{2d_{32}^{p'}(d_{32}^p s_{11}^p - d_{31}^p s_{21}^p)}{k_y w \cot(k_y w / 2)} \right) + [(s_{11}^p s_{22}^p - s_{12}^p s_{21}^p) \epsilon_{33}^T - s_{22}^p (d_{31}^p)^2 - s_{11}^p (d_{32}^p)^2 + (s_{12}^p + s_{21}^p) d_{31}^p d_{32}^p]}$$

Similarly, the transverse ME coefficient $\alpha_{E32} = \delta E_3 / \delta H_2$ is given by

$$\alpha_{E32} = \frac{\left(\frac{2q_{21}^{m'}(d_{32}^p s_{12}^p - d_{31}^p s_{22}^p)}{k_x l \cot(k_x l / 2)} + \frac{2q_{22}^{m'}(d_{31}^p s_{21}^p - d_{32}^p s_{11}^p)}{k_y w \cot(k_y w / 2)} \right)}{\left(\frac{2d_{31}^{p'}(d_{31}^p s_{22}^p - d_{32}^p s_{12}^p)}{k_x l \cot(k_x l / 2)} + \frac{2d_{32}^{p'}(d_{32}^p s_{11}^p - d_{31}^p s_{21}^p)}{k_y w \cot(k_y w / 2)} \right) + [(s_{11}^p s_{22}^p - s_{12}^p s_{21}^p) \epsilon_{33}^T - s_{22}^p (d_{31}^p)^2 - s_{11}^p (d_{32}^p)^2 + (s_{12}^p + s_{21}^p) d_{31}^p d_{32}^p]}$$

The above equations correspond to a special case of the ME theory in which the anisotropic piezoelectric properties ($s_{11}^p \neq s_{22}^p, s_{12}^p = s_{21}^p$ and $d_{31}^p \neq d_{32}^p$) are considered with $l \neq w$. One can check the validity of the above equations by solving the above equations for isotropic 2D laminate with isotropic piezoelectric properties. After putting the isotropic piezoelectric material parameters $s_{11}^p = s_{22}^p, s_{12}^p = s_{21}^p, d_{31}^p = d_{32}^p$ in the Eqs. (18) and (19) one can get,

$$\alpha_{E31} = - \frac{\left(\frac{q_{11}^{m'}}{k_x l \cot(k_x l / 2)} + \frac{q_{12}^{m'}}{k_y w \cot(k_y w / 2)} \right)}{\left(\frac{d_{31}^{p'}}{k_x l \cot(k_x l / 2)} + \frac{d_{31}^{p'}}{k_y w \cot(k_y w / 2)} \right) + \frac{\epsilon_{33}^T}{X} \left[1 - \frac{X(d_{31}^p)}{\epsilon_{33}^T} \right]} \quad (20)$$

$$\text{with } X = \frac{2d_{31}^p}{(s_{11}^p + s_{12}^p)}$$

The above equation is in good agreement with the theory derived by Bao and Luo²⁵ for the 2D isotropic ME laminate. Note that the coordinate system and notation of the physical terms in above equations have been changed from the original version²⁵ to be consistent with our case.

Similarly one can find the equation for 1D isotropic laminate with length l much larger than width w and thickness t ,⁹

$$\alpha_{E31} = \left(\frac{d_{31}^p q_{11}^m s_{12}^p \tan(kl/2)}{s_2 [2(d_{31}^p)^2 - (s_{11}^p + s_{12}^p) \epsilon_{33}^T] kl - (d_{31}^p)^2 s_{12}^m \tan(kl/2)} \right) \quad (21)$$

with $s_2 = \frac{s_{12}^m + s_{12}^p}{2}$. The above Eq. (21) is not fully consistent with the reported one in ref. [9]

if we assume $f = 0.5$ and the effective permeability $\mu = 1$. This implies that the transverse stress should be considered even though the sample is 1D like.

From Eqs. (18) and (19), we can clearly find two different resonance frequencies likely due to the difference in the elastic compliances of the Piezoelectric materials, which have never been reported before.

$$f_{r1} = \frac{1}{2l} \sqrt{\left(\frac{1-f}{s_{11}^p} + \frac{f}{s_{11}^m} \right) / \bar{\rho}}$$

$$f_{r2} = \frac{1}{2l} \sqrt{\left(\frac{1-f}{s_{22}^p} + \frac{f}{s_{11}^m} \right) / \bar{\rho}} \quad (22)$$

III. NUMERICAL SIMULATION OF THEORY

Based on the above theory, we have done the numerical calculations for the transverse ME voltage coefficient both at low and resonance frequency. In case of the low frequency ME effect, the calculations were performed by using the material parameter given in Table 1 into Eqs. (5) and (6). The calculated values of α_{E31} and α_{E32} are found to be 3.451 and -4.572 V/cmOe, respectively, showing opposite signs and different magnitudes. Moreover, the anisotropy ratio is found to be ~ 0.75 . However, this anisotropic behavior has never been reported before and cannot be explained by the theoretical expression for isotropic ME laminates.

Similarly, the frequency dependence of α_{E31} and α_{E32} are calculated by using Eqs. (18) and (19) with square symmetric laminate, $l = w$. The numerical simulation data of Eqs. (18) and (19) were given in the Figs. 2(a) and 2(b). From the figures it can be seen that both α_{E31} and α_{E32} show two strong resonance peaks at $f_1 = 176$ kHz and $f_2 = 205$ kHz. Moreover, the phase change is observed between α_{E31} and α_{E32} as shown in Fig. 2(b). At low frequencies α_{E31} maintains a small positive value. When the frequency is increased to pass the resonant frequency, α_{E31} shows a positive peak and a negative dip structure successively. In contrast, the phase of α_{E32} changed by 180 degree. Namely, α_{E32} showed successively a negative dip and a positive peak structure. On the other hand, the ratio of $|\alpha_{E31}/\alpha_{E32}|$ was overall frequency dependent, showing drastic changes near the resonant frequencies. The ratio is found to be 0.62 at frequency f_1 while it is 1.5 at f_2 . Moreover, we found that the ratio is very sensitivity with small changes of the material parameters.

IV. COMPARISON OF NUMERICAL SIMULATION WITH EXPERIMENTAL RESULTS

To verify the proposed theoretical models, we have compared the numerical simulations with the experimental data. Measurements were done on the symmetric Ni/PMN-PT/Ni laminates with lateral dimensions of $10 \times 10 \text{ mm}^2$ by use of [011] oriented single crystals of PMN-PT. High quality PMN-PT ($0.7\text{Pb}(\text{Mg}_{1/3}\text{Nb}_{2/3})\text{O}_3-0.3\text{PbTiO}_3$) single crystals were grown by the Bridgeman method (IBULE Photonics, Korea) and cut in a planar shape with a thickness of 0.3 mm oriented along [011] direction (Fig. 1(b)). The ME laminates were prepared by stacking six Ni layers (Alfa Aesar, 99.9%), of which thickness is 0.15 mm on the top and bottom surfaces of the PMN-PT using a silver epoxy. The samples were poled by applying a dc electric field of 10 kV/cm. To investigate quantitatively the ME coupling, a magnetoelectric susceptometer, working at both resonant and low frequency conditions, was used. A pair of Helmholtz coils was used to generate AC magnetic field δH_{ac} in a broad frequency range ($f=194 \text{ Hz}-1 \text{ MHz}$) and the resultant AC voltage across the sample was measured by a lock-in amplifier as a function of H_{dc} to estimate a complex ME voltage coefficient $\tilde{\alpha}_E \equiv \alpha_E + i \text{Im}(\tilde{\alpha}_E)$. The material parameters for each phases have been given in the following Table 1.

Figure 3 presents α_E curves of the laminate with [011]-cut crystal measured at $f=194 \text{ Hz}$ for $H_{dc}//[100]$ and $//[0\bar{1}1]$. For both H_{dc} directions, α_E exhibits a typical H_{dc} dependence showing a sign change with respect to the reversal of H_{dc} direction. Moreover, α_E values along $H//[0\bar{1}1]$ and $H//[100]$ clearly show opposite signs and the maximum magnitudes become 0.64 and 1.92 V/cmOe, respectively, constituting their ratio of ~ 0.34 , being consistent with the theoretical calculations. The theory and the experiments are in good agreement with each other. The difference between this value and the experimental data might be due to the use of the published

data available in the literature while the parameters specific to our PMN-PT and Ni might be a bit different.

Similarly, we have measured the frequency dependence of $|\tilde{\alpha}_E|$ for the laminate with [011]-oriented PMN-PT (Fig. 4(a)), finding two strong $|\tilde{\alpha}_E|$ peaks at $f_1 = 183$ kHz and $f_2 = 217$ kHz for both $H//[0\bar{1}1]$ and $H//[100]$. Moreover, the magnitude of each $|\tilde{\alpha}_E|$ peak is different for the two H directions. Moreover, the phase difference of 180 degree is observed for α_E for different H directions, as shown in Fig. 4(b). The experimental results show good agreement with the theoretical simulations. However, the experimental ratio is consistent over the wide frequency range, being inconsistent with the theoretical calculations.

The present theory can clearly explain the anisotropy and multi-frequency behaviour observed in the ME laminate with anisotropic piezoelectric materials, however the ratio of $|\alpha_{E31}/\alpha_{E32}|$ showed inconsistency between the theoretical and experimental results. The difference in the theoretical ratio over wide frequency range can be expected as it is strongly influenced by the small changes in the material parameters. The material parameters used in the present calculations are not ideal while they might be different for PMN-PT and Ni. More importantly, it should be noted that in the real ME laminate structure, there are energy losses, which have not been taken into account in the present theory. Moreover, even in perfect materials, in the absence of other types of losses, there are losses associated with the presence of an electrical contact. These losses determine the resonance line width and the maximum value of the magnetoelectric voltage coefficient.

In conclusion, theoretical models for the transverse ME voltage coefficients at low and resonance frequency were derived. Our theoretical models provide two different sets of equations of transverse ME voltage coefficients for different in-plane magnetic fields. The theoretical calculations indicate that the ME voltage coefficients are strongly dependent on the anisotropic piezoelectric coefficients and elastic compliances of piezoelectric PMN-PT crystal. The theoretical simulations show consistency with the experimental results, accounting the validity of the theoretical models. Our theoretical modeling should be generally applicable to other ME laminates with any piezoelectric with anisotropic piezoelectric coefficients. The theory can help us to optimize the different material parameters in order to further enhance the ME voltage coefficients.

References

- ¹N. A. Spaldin and M. Fiebig, *Science* **309**, 391 (2005).
- ²M. Fiebig, *J. Phys. D: Appl. Phys.* **38**, R123 (2005).
- ³P. Li, Y. Wen, P. Liu, X. Li, and C. Jia, *Sens. Actuators A.* **157**, 100 (2010).
- ⁴Y. K. Fetisov, A. A. Bush, K.E. Kamentsev, A.Y. Ostashchenko, and G. Srinivasan, *IEEE Sens.* **6**, 935 (2006).
- ⁵S. X. Dong, J. Y. Zhai, J. F. Li, D. Viehland, and M. I. Bichurin, *Appl. Phys. Lett.*, **89**, 243512 (2006).
- ⁶S. X. Dong, J. F. Li, and D. Viehland, *Appl. Phys. Lett.* **83**, 2265 (2003).
- ⁷G. Harshe, J. O. Dougherty, and R. E. Newnham, *Int. J. Appl. Electromagn. Mater.* **4**, 145 (1993).
- ⁸M. I. Bichurin, V. M. Petrov, and G. Srinivasan, *J. Appl. Phys.* **92**, 7681 (2002).
- ⁹M. I. Bichurin, V. M. Petrov, S. V. Averkin, and A. V. Filippov, *Phys. Solid State.* **52**, 2116 (2010).
- ¹⁰S. Priya, R. Islam, S. Dong, and D. Viehland, *J. Electroceram.* **19**, 147 (2007).
- ¹¹C. W. Nan, M. I. Bichurin, S. X. Dong, D. Viehland, and G. Srinivasan, *J. Appl. Phys.* **103**, 031101 (2008).
- ¹²J. Ma , J. Hu , Z. Li , and C. W. Nan, *Adv. Mater.* **23**, 1062 (2011).
- ¹³G. Srinivasan, *Annu. Rev. Mater. Res.* **40**, 153 (2010).
- ¹⁴J. Gao, L. Shen, Y. Wang, D. Gray, J. Li, and D. Viehland, *J. Appl. Phys.* **109**, 074507 (2011).
- ¹⁵Y. Chen, A. L. Geiler, T. Fitchorov, C. Vittoria, and V. G. Harris, *Appl. Phys. Lett.* **95**, 182501 (2009).
- ¹⁶C.-S. Park, K.-H. Cho, M. A. Arat, J. Evey, and S. Priya, *J. Appl. Phys.* **107**, 094109 (2010).

- ¹⁷R. C. Kambale, D.-Y. Jeong, and J. Ryu, *Adv. Cond. Matt. Phys.* **2012**, 824643 (2012).
- ¹⁸K. H. Cho and S. Priya, *Appl. Phys. Lett.* **98**, 232904 (2011).
- ¹⁹C. W. Nan, M. I. Bichurin, S. X. Dong, D. Viehland, and G. Srinivasan, *J. Appl. Phys.* **103**, 031101 (2008).
- ²⁰M. I. Bichurin, V. M. Petrov, S. V. Averkin, and E. Liverts, *J. Appl. Phys.* **107**, 053904 (2010).
- ²¹G. Srinivasan, E. T. Rasmussen, and R. Hayes, *Phys. Rev. B* **67**, 014418 (2003).
- ²²C.-W. Nan, G. Liu, Y. Lin, and H. Chen, *Phys. Rev. Lett.* **94**, 197203 (2005).
- ²³J. L. Dong and S. X. Dwight Viehland, *IEEE Trans. Ultrason. Ferroelectr. Freq. Control* **51**, 794 (2004).
- ²⁴Y. Wang, D. Hasanyan, M. Li, J. Gao, J. Li, D. Viehland, and H. Luo, *J. Appl. Phys.* **111**, 124513 (2012)
- ²⁵B. Bao and Y. Luo, *J. Appl. Phys.* **109**, 094503 (2011)
- ²⁶H. Cao, V. H. Schmidt, R. Zhang, W. Cao, H. Luo, *J. Appl. Phys.* **96**, 549 (2004).
- ²⁷P. F. Wang, L. Luo, D. Zhou, X. Zhao, and H. Luo, *Appl. Phys. Lett.* **90**, 212903 (2007).
- ²⁸Y. K. Fetisov, V. M. Petrov, and G. Srinivasan. *J. Mater. Res.* **22**, 2074 (2007)
- ²⁹B. Zadov, A. Elmalem, E. Paperno, I. Gluzman, A. Nudelman, D. Levron, A. Grosz, S. Lineykin, and E. Liverts, *Adv. Cond. Matt. Phys.* **2012**, 383728 (2012).

FIGURE CAPTIONS:

FIG. 1. (a) A thin ME laminate and defined Cartesian coordinates and (b) Schematic of PMN-PT single crystals with [011]-orientation. Out of 8 possible polarization directions inherent to the rhombohedral symmetry, 2 polarization directions are chosen for Cut-Bupon poling (red dotted lines).

FIG. 2. Numerical simulation of frequency dependence of (a) the modulus of ME voltage coefficient i.e., $|\alpha_E|$ along different H directions and of (b) real component of ME voltage coefficient i.e., α_E for the Ni/[011]-PMN-PT/Ni laminate.

FIG. 3. H_{dc} dependence of α_E at a frequency $f=194$ Hz for Ni/[011]-PMN-PT/Ni laminates.

FIG. 4. Experimental results of frequency dependence of (a) the modulus of ME voltage coefficient i.e., $|\alpha_E|$ along different H directions and of (b) real component of ME voltage coefficient i.e., α_E for the Ni/[011]-PMN-PT/Ni laminate.

Table 1: Material parameters for Ni and [011]-oriented PMN-PT single crystal used for theoretical modelling.

Materials	S_{11}^p or S_{11}^m (10^{-12} m ² /N)	S_{22}^p or S_{22}^m (10^{-12} m ² /N)	S_{12}^p or S_{12}^m (10^{-12} m ² /N)	g_{11} (10^{-9} m/A) or d_{31} (10^{-12} C/N)	g_{22} (10^{-9} m/A) or d_{32} (10^{-12} C/N)	g_{12} (10^{-9} m/A)	ϵ_{33}/ϵ_0
Ni ^a	4.57	-	-1.37	1.25	-	-0.59	-
[011]PMNPT ^c	18	112	-31.1	610	-1883	-	4003

^aCited from Ref. 28, 29 .

^bCited from Ref. 26.

^cCited from Ref. 27.

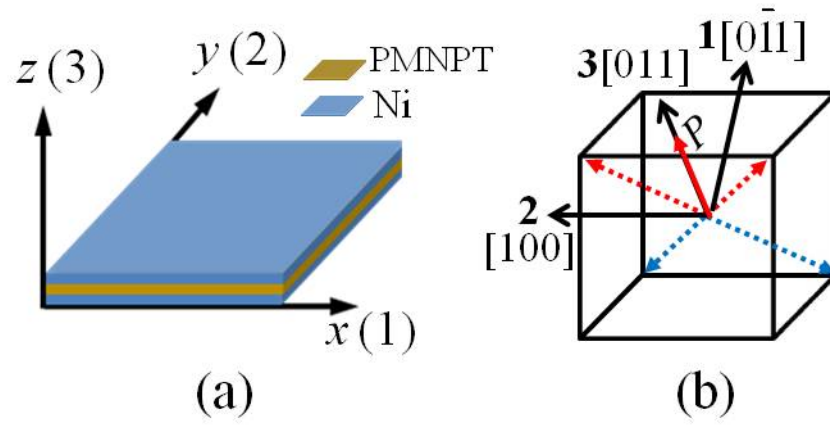


FIG. 1.

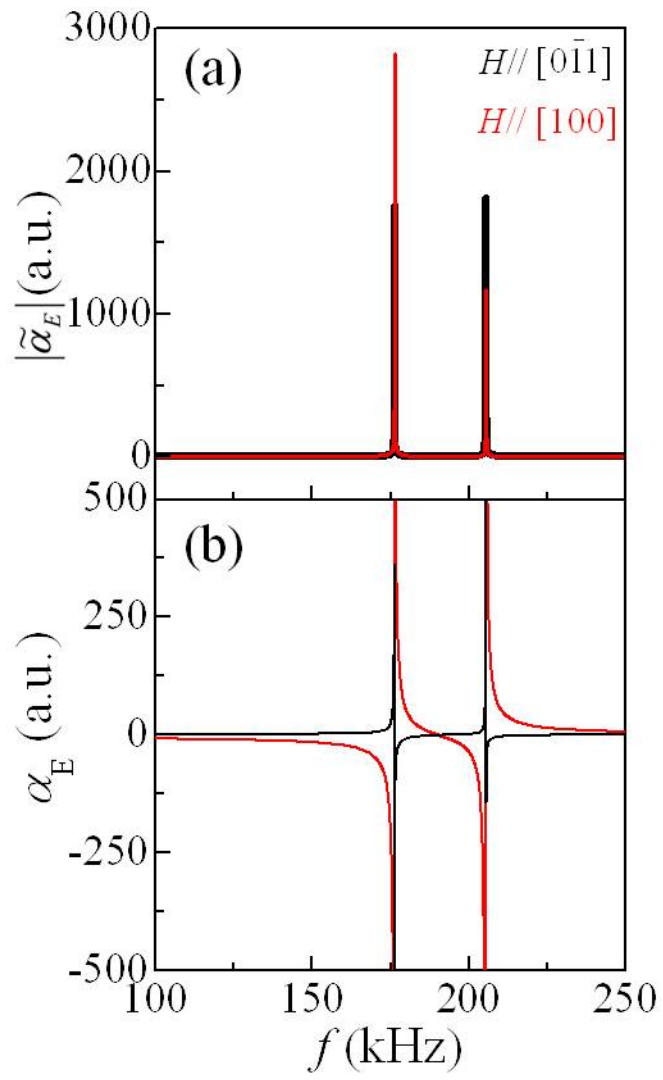


FIG. 2.

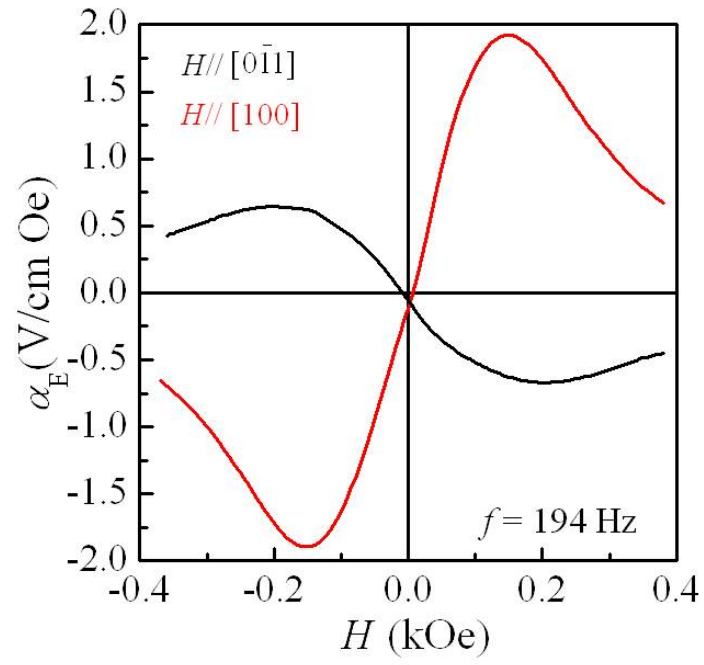


FIG. 3.

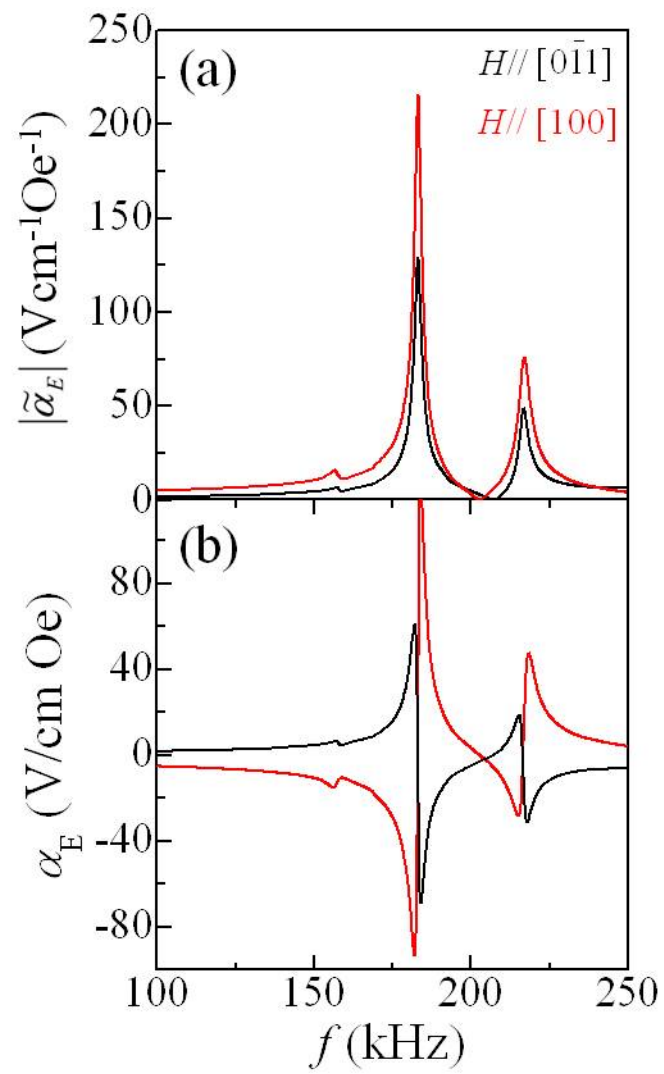


FIG. 4.